applied sciences

MDPI

Article

A Novel Measurement Method for Determining Geometric Errors of Rotary Tables by Using LaserTRACER and Reflectors

Chi-Hua Hsu [1], Jr-Rung Chen [1], Fan-Hsi Hsu [2] and Yu-Ta Chen [3,*]

[1] Center for Measurement Standards, Industrial Technology Research Institute, Hsinchu 30011, Taiwan
[2] Department of Semiconductor and Electro-Optical Technology, Ming-Hsin University of Science and Technology, Hsinchu 30401, Taiwan
[3] Department of Mechanical Design Engineering, National Formosa University, Yunlin 632301, Taiwan
* Correspondence: YuTaChen@nfu.edu.tw

Abstract: In this paper, a novel and robust measurement method is proposed for obtaining the geometric errors of rotary tables by using LaserTRACER and the reflectors mounted on the reflector standard fixture. For the machining accuracy, the six-degree-of-freedom (6-DOF) geometric errors of the rotary axes interactively influence the manufacturing quality of the precise workpieces. Therefore, this paper mainly aims to develop a measurement method for identifying the 6-DOF geometric errors of rotary tables without using the external linear axis. Furthermore, the set-up errors of the reflector standard fixture are also considered and identified to reduce the influence of the 6-DOF geometric error measurements. For each rotary table geometric error measurement, the positions of the LaserTRACER as well as the relative distance between the reflectors and the LaserTRACER are measured and obtained for determining the 6-DOF geometric errors of the rotary tables. In addition, the homogeneous transformation matrix (HTM), multilateration method, and least squares method are used for building the mathematical measurement algorithm. Moreover, the experimental verifications are implemented to demonstrate the accuracy of the proposed measurement method. Conclusively, the experiment and simulation verification results clearly delineate that the maximal relative differences in the linear errors and the angular errors of the 6-DOF geometric errors are, at most, 3.25% and 2.30%, respectively.

Keywords: rotary table; geometric errors; multilateration method; auto-tracking laser interferometer

Citation: Hsu, C.-H.; Chen, J.-R.; Hsu, F.-H.; Chen, Y.-T. A Novel Measurement Method for Determining Geometric Errors of Rotary Tables by Using LaserTRACER and Reflectors. *Appl. Sci.* **2023**, *13*, 2419. https://doi.org/10.3390/app13042419

Academic Editors: Minvydas Ragulskis, Wen-Hsiang Hsieh and Jia-Shing Sheu

Received: 28 December 2022
Revised: 9 February 2023
Accepted: 10 February 2023
Published: 13 February 2023

1. Introduction

In the modern manufacturing industry, ultra-precision multi-axis machining has become the most important development direction [1,2]. In addition, along with the increasing need for workpieces with complex geometries, the demand for multi-axis CNC machine tools has significantly increased in recent years [3,4]. With regard to the efficiency and convenience of manufacturing, multi-axis machine tools with rotary tables have superior characteristics, such as the ability to aid in manufacturing deep holes in two different orientations [5–7]. Moreover, many workpieces with precise angular specifications, such as polyhedrons, are machined through tilting and rotating the rotary tables to meet the requirements for precise positioning and orientation. Therefore, among the multi-axis machine tools, the five-axis CNC machine tools are more widely applied than three-axis CNC machine tools because they have two additional rotary axes. However, the performance of rotary tables immediately affects the position and orientation of the tools relative to the workpieces and the machining accuracy of the machine tools [7–9]. In general, 6-degree-of-freedom (6-DOF) geometric errors greatly affect the performance of rotary tables [10,11]. Consequently, how to accurately measure and identify the 6-DOF geometric errors of rotary tables is particularly important for improving the accuracy of machine tools.

As defined by the International Organization for Standardization (ISO) 230-7, the position-independent geometric errors (PIGEs) and position-dependent geometric errors

(PDGEs) of a rotary axis are described as location and component errors, respectively [12–14]. In ISO 10791-1 to 10791-3, quasi-static tests to calibrate the static errors of the axis average line of rotary axes have been proposed [15–17]. Furthermore, for measuring the position and orientation errors of rotary axes in five-axis machine tools, ISO 10791-6 presents dynamic interpolation tests that use the double ball-bar or the R-test [18,19]. Although the measurement methods mentioned in these ISO standards are effective for identifying the geometric errors of the rotary axes, they lack efficiency and the automated calibration procedures that embody the spirit of Industry 4.0 [7,20].

Over the past few decades, many research studies for identifying the geometric errors of rotary axes have been reported that use double ball-bar (DBB), touch-trigger probes and their artifacts, and geometrical optics methods, as well as interferometry techniques [21–23]. For example, Jiang et al. used the double ball-bar (DBB) to identify PIGEs in rotary axes of a five-axis machine tool by establishing specific testing paths [24]. Furthermore, Xia et al. presented a decoupled method to identify the PIGEs and PDGEs of a rotary axis based on a double ball-bar [25]. By using touch-trigger probes and their artifacts, Ibaraki et al. proposed a series of schemes to calibrate the error map and the location errors of rotary axes with on-the-machine measurements of test pieces [20,26]. In our earlier research, a set of methodologies was also proposed for measuring the PIGEs and PDGEs of rotary axes by using a probe and artifacts. In addition, based on geometrical optics methods, He et al. proposed a dual optical path measurement method (DOPMM) to identify error parameters in the rotary axis of a machine tool by using two precise laser displacement sensors and a self-designed fixture [27]. A single-mode fiber-coupled laser and two retroreflectors were adopted by Li et al. for simultaneously measuring 5-DOF motion errors of a rotary axis [28].

In recent years, with the rapid development of interferometry techniques, there has been many studies proposing geometric error methodologies for rotary axes that use laser interferometers. Using laser interferometers for measuring geometric errors in machine tools has two advantages: (1) a larger angle measurement range, and (2) minimizing the error influences during measurement [9,29]. According to the literature, the interferometer-based machine tool geometric error measurement technology can be mainly divided into two methods: laser tracker-based measurement methods and laser tracer-based measurement methods [30,31]. Regarding laser tracker-based measurement methods, Zhang et al. proposed a general method based on point measurements for identifying the geometric errors of multi-axis machine tools [32]. Li et al. also used a laser tracker to propose a novel principle: a pose measurement principle to realize the precise calibration of a numerical control (NC) machine tool [33]. The time-sharing measurement principle as well as the multi-station methods were proposed to identify the relative position relationship between the rotary and linear axes of a multi-axis NC machine tool by using a laser tracker [34]. As mentioned above, the single-base station and multi-base station measurement methods of using the laser trackers for measuring the geometric errors of machine tools have been widely used. Using laser trackers for machine tool geometric error measurements has advantages, as they are low cost and easy to set up; nevertheless, the measurement accuracy is limited by the measurement principles and the encoder of the rotary axes in the laser tracker. As a result, in order to address this issue, the LaserTRACER was designed by researchers at the Physikalisch-Technische Bundesanstalt (PTB) and the National Physical Laboratory (NPL) [35–37]. Compared to the laser tracker-based measurement methods, the laser tracer-based measurement methods have more precise characteristics due to them having a measurement algorithm and mechanism. As a result, for identifying the geometric errors of the machine tools more precisely, the laser tracer-based measurement methods have become much more popular and are utilized in high-precision machine tool manufacturing [38].

Therefore, based on laser tracer-based measurement methods, this paper proposes a novel measurement method to identify the 6-DOF geometric errors of rotary tables by using LaserTRACER and reflectors. Based on the multilateration method, homogeneous transformation matrix (HTM), and least squares method, the mathematical measurement

algorithm is built for calculating the 6-DOF geometric errors of rotary tables. In addition, the set-up errors of the reflector standard fixture that affect the geometric error measurement accuracy are also considered and identified. Finally, verification of the simulation and experiment is executed by using LaserTRACER and the reflectors, which are mounted on the reflector standard fixture.

2. Measurement Principles

Due to the requirement for high measurement accuracy, the principles of multi-station and time-sharing measurements developed by Wang et al. were adopted and improved in this paper to obtain and identify the 6-DOF geometric errors of rotary tables [33,39]. In addition, to obtain the spatial coordinate position of the LaserTRACER and the reflectors, the multilateration method was also adopted in this paper [30,31]. The multilateration method was proposed by Takatsuji et al. by solving a set of four equations [40,41]. Accordingly, the positions of the LaserTRACER and the reflectors were identified through the measurement principle and are depicted in this section.

Since the detailed mathematical derivation of the multilateration method can be found in our previous publications [30,31], this section only reviews it briefly and presents how it is different here. Based on laser interferometry techniques, the operation principle of the LaserTRACER only involves the length measurement. When the LaserTRACER was placed at each base station, the distances between the LaserTRACER and each reflector position were obtained and recorded sequentially. As a result, the position of each LaserTRACER base station can be calculated and obtained through Equation (1):

$$l_{ij} + l_{oj} + r_{ij} = s_j \sqrt{(x_i - x_{0j})^2 + (y_i - y_{0j})^2 + (z_i - z_{0j})^2}, \quad (1)$$

where (x_i, y_i, z_i) represents the coordinate position of the i-th measurement point; (x_{0j}, y_{0j}, z_{0j}) represents the coordinate position of the j-th LaserTRACER; when the reflector is located at the i-th measurement point, l_{ij} is the measured length; l_{0j} is the initial distance between the reflector and the j-th LaserTRACER; and s_j is the scale factor for the j-th LaserTRACER; finally, r_{ij} is the residual error.

As shown in Figure 1, the reflectors with the reflector standard fixture were mounted on the rotary table, and the LaserTRACER was installed at different base stations externally to the measured rotary table for the 6-DOF geometric error measurements. Moreover, Pi (i = 1–6) in Figure 1 represents the six different LaserTRACER base stations, even though, according to the literature, using four different reflector positions and LaserTRACER base stations are enough to calibrate the 6-DOF geometric errors of a rotary table. However, for a much better convergence of the measurement equations, the original principle of multi-station and time-sharing measurements was improved and utilized in this paper. Consequently, six different reflector positions and six different LaserTRACER base stations were used in this paper to identify the position and orientation of the rotary table.

First, the rotary table (A-axis) was driven to the home position (zero position). When the LaserTRACER was placed at the first base station (P1), the distances between P1 and each reflector were measured. By using Equation (1) and the Levenberg–Marquardt method, the position of the LaserTRACER at the first base station (P1) can be identified. Then, the positions of LaserTRACER base stations P1 to P6 were also obtained sequentially. Second, the rotary table was driven to each measurement position. Afterwards, the distances between each reflector at each measurement position and the LaserTRACER base station were measured. Likewise, the positions of each reflector at each measurement position were also calculated by using Equation (1) and the Levenberg–Marquardt method.

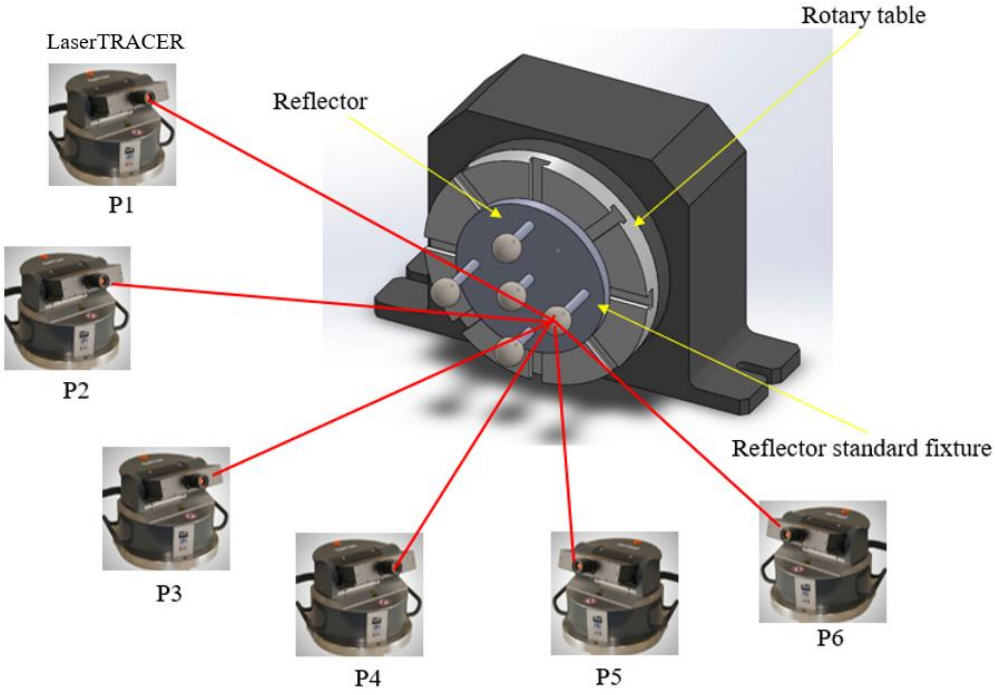

Figure 1. Schematic diagram of the proposed measurement method.

3. Geometric Error Measurement Algorithm

According to the reference ISO 230-7, there are 6-DOF geometric errors in the rotary axis, which are usually caused by defects in component manufacturing [13]. Therefore, using the rotary A-axis as an example, the 6-DOF geometric errors of the A-axis consist of the axial motion error δ_{xa}, the radial motion errors δ_{ya} and δ_{za} in the y and z directions, respectively, and the angular deviations ε_{xa}, ε_{ya} and ε_{za}, around the X-, Y- and Z-axes, respectively. For the purposes of identifying the 6-DOF geometric errors of the rotary table, a measurement algorithm is presented in this subsection through analyzing the deviations of the spatial coordinate positions of the reflectors. It must be emphasized that executing the proposed measurement methodology is not needed to drive the other three linear axes. In other words, the 6-DOF geometric errors of the rotary table can be determined without three-axis machine tools by using the proposed measurement method.

In the ideal case, the central lines of the reflector standard fixture must be located along the average lines of the rotary table during measurement. However, it is difficult to make the reflector standard fixture position and the rotary table position agree within an acceptable tolerance due to installation issues. According to our past experiences, the set-up errors, including two linear offset errors O_{ya} and O_{za} in the y and z directions, respectively, and two the angular errors S_{ya} and S_{za} around the Y- and Z-axes, respectively, affected the accuracy of the measured value. As a result, the set-up errors are identified in Section 3.1.

3.1. Set-Up Error Identification

As expected, the set-up errors of the reflector standard fixture greatly affect the measurement accuracy of the proposed measurement method. In this subsection, the mathematical measurement equations and estimation algorithm are proposed by using HTMs and the least squares method. In the ideal case, a rotary table operates along the prospective path. As a result, the ideal position of each reflector at each prospective measurement point can be estimated by the first measurement position. However, in a real case, the set-up errors of the reflector standard fixture always exist and influence the measurement values when the proposed measurement method is executed for measuring the rotary table geometric errors. According to the results mentioned above, the real positions of the reflectors at each

measurement point are obtained. Consequently, the difference between the ideal and real positions of the reflector at each measurement point is formulated with Equation (2):

$$^{real}P(i,m) = {}^{ideal}P(i,m) + dP^m_{k,i} \quad k \in x,y,z, \tag{2}$$

where $^{real}P(i,m)$ and $^{ideal}P(i,m)$ denote the real and ideal positions of the m-th reflector at the i-th measurement point, respectively. Moreover, $dP^m_{k,i}$ represents the difference between the ideal and real positions of the m-th reflector at the i-th measurement point in the x, y, and z directions. Furthermore, since the higher term has a small impact on the results of Equation (2), a first-order Taylor series expansion method is applied to calculate the difference between the ideal and real positions of the reflector at the i-th measurement point and can be expressed as follows:

$$dP^m_{k,i} = \sum_{t=1}^{4} \frac{\partial P^m_{k,i}}{\partial E_t} \Delta E_t, \tag{3}$$

where E_t represents the four set-up errors of the rotary table depicted above.

When conducting the measurements of the rotary table, the rotary table is driven to the angular position θ_i at the i-th measurement point to identify the real center positions of the reflector. Therefore, the relative equations for determining the difference between the ideal and real positions of the m-th reflector at the i-th measurement point in the x, y, and z directions and the set-up errors of the reflector standard fixture are given as follows:

$$\begin{aligned} dP^m_{k,i} &= \begin{bmatrix} dP^m_{x,1} \\ dP^m_{y,1} \\ dP^m_{z,1} \\ \vdots \\ dP^m_{x,i} \\ dP^m_{y,i} \\ dP^m_{z,i} \end{bmatrix}_{3i} = A_{3i\times 4}E_{4\times 1} \\ &= \begin{bmatrix} 0 & 0 & z^m_1 - z^m_1\cos\theta_1 - y^m_1\sin\theta_1 & -y^m_1 + y^m_1\cos\theta_1 - z^m_1\sin\theta_1 \\ 1-\cos\theta_1 & \sin\theta_1 & 0 & 0 \\ \sin\theta_1 & -1+\cos\theta_1 & 0 & 0 \\ \vdots & \vdots & \vdots & \vdots \\ 0 & 0 & z^m_i - z^m_i\cos\theta_i - y^m_i\sin\theta_i & -y^m_i + y^m_i\cos\theta_i - z^m_i\sin\theta_i \\ 1-\cos\theta_i & \sin\theta_i & 0 & 0 \\ \sin\theta_i & -1+\cos\theta_i & 0 & 0 \end{bmatrix}_{3i\times 4} \begin{bmatrix} O_{ya} \\ O_{za} \\ S_{ya} \\ S_{za} \end{bmatrix} \end{aligned} \tag{4}$$

where the parameters x^m_i, y^m_i and z^m_i represent the spatial coordinate positions of the m-th reflector, respectively.

As shown, Equation (4) is an overdetermined system. As a result, the least squares method is used for estimating the set-up errors of the reflector standard fixture. For approximating the solution of overdetermined systems, a standard mathematical optimization method is built by using the least squares method. Thus, Equation (5), which is related to the least squares method, can be expressed as follows:

$$Q(E_t) = \frac{1}{3i}\sum_{s=1}^{3i}\left(dP^m_{k,i} - AE\right)^2 = \frac{1}{3i}\sum_{s=1}^{3i} R^2_s. \tag{5}$$

In order to identify the optimal set-up errors of the reflector standard fixture, the average of the squared residuals are minimized and expressed in Equation (6):

$$\min_{E_t} \sum_{s=1}^{3i} R_s^2 = \min \left\| dP_{k,i}^m - AE \right\|^2 = \min_{E_t} \left\| \begin{bmatrix} dP_{x,1}^1 \\ \vdots \\ dP_{z,i}^m \end{bmatrix} - \begin{bmatrix} A_{1\times1} & \cdots & A_{1\times4} \\ \vdots & \ddots & \vdots \\ A_{i\times1} & \cdots & A_{i\times4} \end{bmatrix} \begin{bmatrix} O_{ya} \\ O_{za} \\ S_{ya} \\ S_{za} \end{bmatrix} \right\|^2. \quad (6)$$

3.2. 6-DOF Geometric Error Identification

The proposed 6-DOF geometric error measurement algorithm, excluding the influence of the set-up errors of the reflector standard fixture, is depicted as follows: Before the 6-DOF geometric errors at the different angular positions of the rotary table are identified, the expected positions of the m-th reflector at the i-th measurement point, which are considered as influences on the set-up errors, are established. It is important to note that the expected positions of the reflector are calculated according to Equation (2) and the kinematic error model presented in our previous works [7,19]. Therefore, according to the kinematic error model and HTMs, the relationship between the expected and real positions of the m-th reflector at the i-th measurement point is formulated with Equation (7):

$$^{real}P(i,m) = {}^{expected}P(i,m) + d\widetilde{P_{k,i}^m} \quad k \in x,y,z, \quad (7)$$

where $d\widetilde{P_{k,i}^m}$ denotes the difference between the expected position and real position of the m-th reflector at the i-th measurement point in the x, y, and z directions. Similarly, since the magnitudes of the 6-DOF geometric errors of the rotary table are usually very small, the higher term of the 6-DOF geometric errors has only a small impact on the results. Therefore, by using a first-order Taylor series expansion method, the difference between the expected positions and real positions of the m-th reflector at the i-th measurement point in the x, y, and z directions can be expressed as follows:

$$\begin{aligned} d\widetilde{P_{k,i}^m} &= \begin{bmatrix} d\widetilde{P_{x,i}^1} \\ d\widetilde{P_{y,i}^1} \\ d\widetilde{P_{z,i}^1} \\ \vdots \\ d\widetilde{P_{x,i}^6} \\ d\widetilde{P_{y,i}^6} \\ d\widetilde{P_{z,i}^6} \end{bmatrix}_{3i} = A_{16\times8}F_t \\ &= \begin{bmatrix} 0 & z_1\cos\theta_i + y_1\sin\theta_i & z_1\sin\theta_i - y_1\cos\theta_i & 1 & 0 & 0 \\ -z_1\cos\theta_i - y_1\sin\theta_i & 0 & x_1 & 0 & 1 & 0 \\ y_1\cos\theta_i - z_1\sin\theta_i & -x_1 & 0 & 0 & 0 & 1 \\ \vdots & \vdots & \vdots & \vdots & \vdots & \vdots \\ 0 & z_6\cos\theta_i + y_6\sin\theta_i & z_6\sin\theta_i - y_6\cos\theta_i & 1 & 0 & 0 \\ -z_6\cos\theta_i - y_6\sin\theta_i & 0 & x_6 & 0 & 1 & 0 \\ y_6\cos\theta_i - z_6\sin\theta_i & -x_6 & 0 & 0 & 0 & 1 \end{bmatrix}_{18\times6} \begin{bmatrix} \varepsilon_{xa} \\ \varepsilon_{ya} \\ \varepsilon_{za} \\ \delta_{xa} \\ \delta_{ya} \\ \delta_{za} \end{bmatrix} \end{aligned} \quad (8)$$

where F_t represents the 6-DOF geometric errors of the rotary table. For increasing the measurement accuracy and decreasing the influence of uncertainties, the average $Q(F_t)$ of the squared residuals are minimized by using the least squares method, as shown in Equation (9):

$$Q(F_t) = \min_{F_t} \frac{1}{3m} \sum_{n=1}^{3m} R_n^2 = \frac{1}{3m} \sum_{n=1}^{3m} \left(d\widetilde{P_{k,i}^m} - AF_t \right)^2. \quad (9)$$

4. Simulation Verification

In order to verify the accuracy and performance of the proposed measurement method, the simulation verification presented in this section was executed. The accuracy of the measurement algorithm in identifying the set-up errors of the reflector standard fixture

and the 6-DOF geometric errors of the rotary table was verified by using the Matlab R2019a software (The MathWorks, Inc., Natick, MA, USA) to build the simulation model. The differences between the assumed random values and the calculated values of the set-up errors and the 6-DOF geometric errors are estimated for verifying the performance of the proposed measurement method.

In the simulation model, the analyzed error variables including the set-up errors and the 6-DOF geometric errors shown in the equation were substituted with random variables. Therefore, the simulated real positions of the reflector and LaserTRACER could be obtained without using experimental data by using random variables to substitute for errors. By following the measurements, the simulated parsed values of the set-up errors and the 6-DOF geometric errors were calculated with Equations (1)–(8). Furthermore, 100 independent simulations were implemented. As a result, Tables 1 and 2 show the simulation results of the set-up errors of the reflector standard fixture and the 6-DOF geometric errors of the rotary table, respectively. In addition, the two linear offset errors and the two angular errors of the set-up errors were assumed to be 10 μm and 20 arcsec, respectively. Based on the simulation results, the differences between the linear offset errors and the angular errors were equal to, at most, 4.5% and 4.35%, respectively. On the other hand, the linear errors and the angular errors of the 6-DOF geometric errors were assumed to be random variables from −10 μm to 10 μm and from −20 arcsec to 20 arcsec. As shown in Table 2, the maximal differences in the linear errors and the angular errors were, at most, 3.25% and 2.30%, respectively. Conclusively, the simulation verification demonstrated that the proposed measurement method was feasible and accurate enough for identifying the 6-DOF geometric errors of a rotary table without using three-axis machine tools.

Table 1. Simulation results of set-up errors.

	O_{ya}	O_{za}	S_{ya}	S_{za}
Unit	μm	μm	arcsec	arcsec
Given value	10	10	20	20
Estimated value	9.55	10.35	20.87	19.15
Absolute difference (μm/arcsec)	0.45 μm,	0.35 μm,	0.87″,	0.85″,
Relative difference (%)	4.5%	3.5%	4.35%	4.25%

Table 2. Simulation results of 6-DOF geometric errors.

Symbol	Unit	Range of Given Value	Average Difference
δ_{xa}	μm	±10	0.65 μm, 3.25%
δ_{ya}	μm	±10	0.49 μm, 2.45%
δ_{za}	μm	±10	0.34 μm, 1.70%
ε_{xa}	arcsec	±20	0.92 arcsec, 2.30%
ε_{ya}	arcsec	±20	0.67 arcsec, 1.68%
ε_{za}	arcsec	±20	0.41 arcsec, 1.02%

5. Experiment Verification

As shown in Figure 2, the proposed measurement method was demonstrated on a commercial rotary table and executed by using the LaserTRACER (etalon AG, Braunschweig, Germany) and the reflector standard fixture with the reflectors. The validation experiment for the feasibility and performance of the proposed measurement system was executed using the LaserTRACER and the laboratory-built prototype of the reflector standard fixture. Furthermore, a comparison test was also implemented by using a traditional dial indicator method and the proposed measurement method.

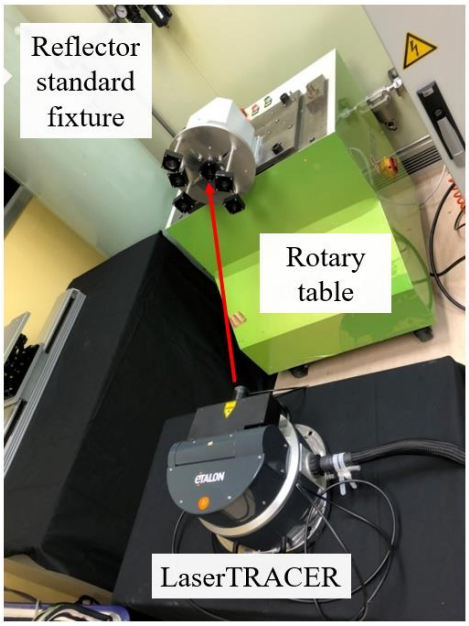

Figure 2. Experimental setup.

5.1. Geometric Error and Set-Up Error Identification Experiment

As shown in Figure 3, the laboratory-built prototype of the reflector standard fixture with reflectors was designed and presented. To obtain and identify the 6-DOF geometric errors of the rotary table more precisely and robustly, it was important to note that the reflector standard fixture was designed for the placement of six non-coplanar holders. In addition, obtaining the relative spatial coordinate positions of the reflectors was important for identifying the LaserTRACER positions. As a result, the relative spatial coordinate positions of the six holders in the reflector standard fixture were measured with the Leitz Ultra coordinate measuring machine (MPE: 0.4 + 1.176 $\times 10^{-7}L$ µm). Table 3 shows the measured data of the six holder positions. In this regard, evaluating the uncertainty associated with the measured data was a must. Since a detailed mathematical derivation can be found in our previous publication and ISO/IEC Guide 98-3:2008, we only briefly review them here and present the results of the measurement uncertainty [7,19,42]. According to ISO/IEC Guide 98-3:2008, the influential factors such as the temperature variation in the reflector standard fixture, repeatability, and the maximum permissible error (MPE) of the coordinate measuring machine (CMM) were considered to estimate the measurement uncertainty. Based on the expression of measurement uncertainty described in [7,42], the combined standard uncertainty $u_c(\Delta L)$ was defined as follows:

$$u_c(\Delta L) = \sqrt{\left(\left|\frac{\partial \Delta L}{\partial \delta_{\text{thermal}}}\right| u(\delta_{\text{thermal}})\right)^2 + \left(\left|\frac{\partial \Delta L}{\partial \delta_{\text{repeatability}}}\right| u(\delta_{\text{repeatability}})\right)^2 + \left(\left|\frac{\partial \Delta L}{\partial \delta_{\text{mpe}}}\right| u(\delta_{\text{mpe}})\right)^2}, \quad (10)$$

where $u(\delta_{\text{thermal}})$, $u(\delta_{\text{repeatability}})$, and $u(\delta_{\text{mpe}})$ represent the standard uncertainties of the temperature variation, repeatability, and MPE of the CMM, respectively. Considering the temperature variation in the reflector standard fixture, repeatability and MPE of the CMM during measurement, the standard uncertainties $u(\delta_{\text{thermal}})$, $u(\delta_{\text{repeatability}})$, and $u(\delta_{\text{mpe}})$ were calculated as 3.12 $\times$ $10^{-7}L$ µm, 0.0289 µm, and 0.4 + 1.176 $\times 10^{-7}L$ µm, respectively. The combined standard uncertainty $u_c(\Delta L)$ can be expressed with Equation (11). Furthermore, based on a 95% confidence level, the coverage factor k = 2, and the expanded measurement uncertainty equation $U = k \times u_c$, the expanded measurement

uncertainty can be expressed as Equation (12). Consequently, Table 3 shows the measured data of the six holder positions with the expanded measurement uncertainty.

$$u_c(\Delta L) = \sqrt{0.401^2 + (3.32 \times 10^{-7} L)^2}. \quad (11)$$

$$U = 2 \times \sqrt{0.401^2 + (3.32 \times 10^{-7} L)^2} \quad (12)$$

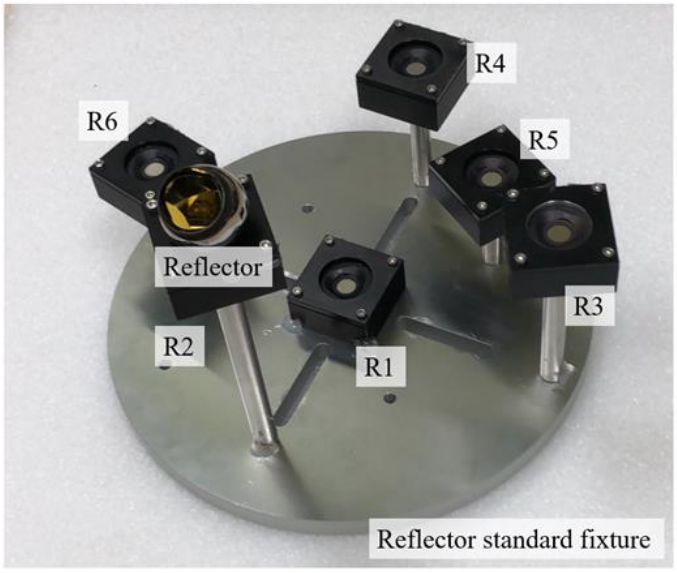

Figure 3. Laboratory-built prototype of reflector standard fixture.

Table 3. Measured data of six holder positions.

	x (mm)	*y* (mm)	*z* (mm)
R1	0	0	0
R2	152.3164 ± 0.00081	99.5804 ± 0.00080	3.1107 ± 0.00080
R3	101.3756 ± 0.00080	−4.1159 ± 0.00080	124.6657 ± 0.00081
R4	75.0115 ± 0.00080	−104.496 ± 0.00080	−3.2143 ± 0.00080
R5	50.72 ± 0.00080	3.6551 ± 0.00080	−115.3568 ± 0.00081
R6	50.7571 ± 0.00080	−65.6545 ± 0.00080	65.1476 ± 0.00080

The complete flowchart of geometric error and set-up error identification experiments is shown in Figure 4. Following the flowchart depicted in Figure 4, the reflector standard fixture with reflectors was firstly put on the rotary table, and then the LaserTRACER was placed in front of the rotary table, as shown in Figure 2. As described in Section 2, the positions of the LaserTRACER at base stations P1 to P6 and the reflector at each measurement position were obtained sequentially during the measurement experiment. Furthermore, based on the equations mentioned in Section 3 and the measured data obtained in this section, six geometric errors from the rotary table and four set-up errors were obtained. Table 4 shows the measured results of the set-up errors of the reflector standard fixture. As shown, the maximum linear offset error and angular error were 192.6 μm and 108.70 arcsec. Furthermore, the linear errors and the angular errors of the 6-DOF geometric errors for the rotary table are shown in Figure 5a,b, respectively.

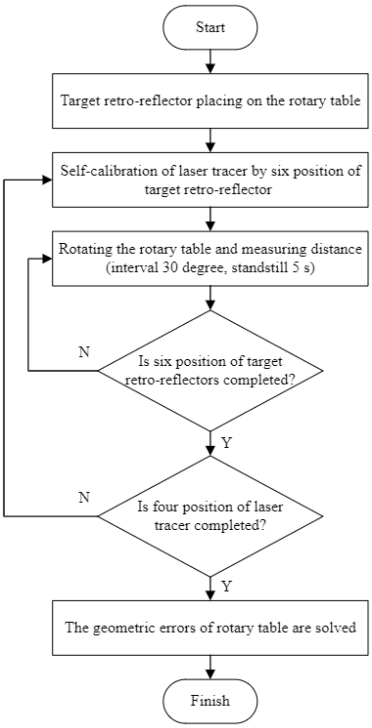

Figure 4. Flowchart of measurement experiment.

Table 4. Measured results of set-up errors.

	O_{ya}	O_{za}	S_{ya}	S_{za}
Unit	μm	μm	arcsec	arcsec
Measured value	59.4	192.6	12.78	108.70

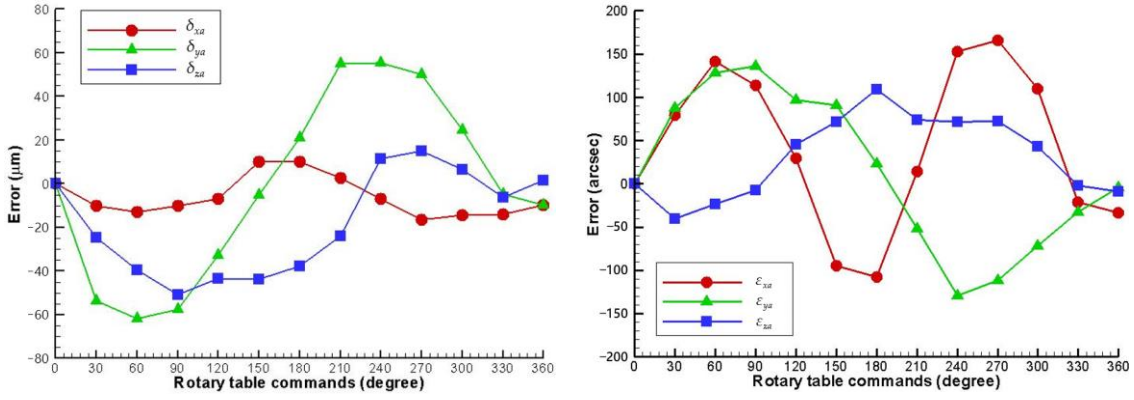

(**a**) (**b**)

Figure 5. Identified geometric errors of rotary table (**a**) linear errors and (**b**) angular errors.

5.2. Verification with Traditional Measurement Method

Until now, there has not been any commercial measurement system available for identifying the 6-DOF geometric errors of rotary tables without using three-axis machine tools. As a result, a comparison test was performed by using the traditional dial indicator method and the proposed measurement method. Figure 6 shows the verification experiment when using the traditional dial indicator method for rotary table measurements. However, the dial indicator is only capable of measuring in a specific direction. In other words, the real positions of the rotary table in the x, y, and z directions can be measured and obtained only by using the dial indicator method. As a result, the comparative test results

of the proposed measurement method and the dial indicator method are shown in Figure 7. Moreover, for evaluating the effectiveness of the proposed measurement method, the E_n-score is adopted for estimating how closely the proposed measurement method agrees with the traditional measurement method. According to ISO 13528 [43], the E_n-score of the measurement results in the x, y, and z directions can be expressed as follows:

$$E_n(k) = \frac{(x_i - \overline{X})}{\sqrt{U_{x_i}^2 + U_{\overline{X}}^2}}, k \in x, y, z, \tag{13}$$

where x_i and $\overline{X}$ denote the measurement results from the proposed and traditional measurement methods, respectively, U_{x_i} and $U_{\overline{X}}$ represent the expanded uncertainty of the measurement results from the proposed and traditional measurement methods. Accordingly, the average of the absolute value of the E_n-score in the x, y, and z directions is 0.77, 0.39, and 0.32, respectively. As shown for the calculated results, all the averages of the absolute values of the E_n-score are below 1. Accordingly, the comparison verification results indicate that the proposed measurement method is feasible and effective for identifying the 6-DOF geometric errors of rotary tables.

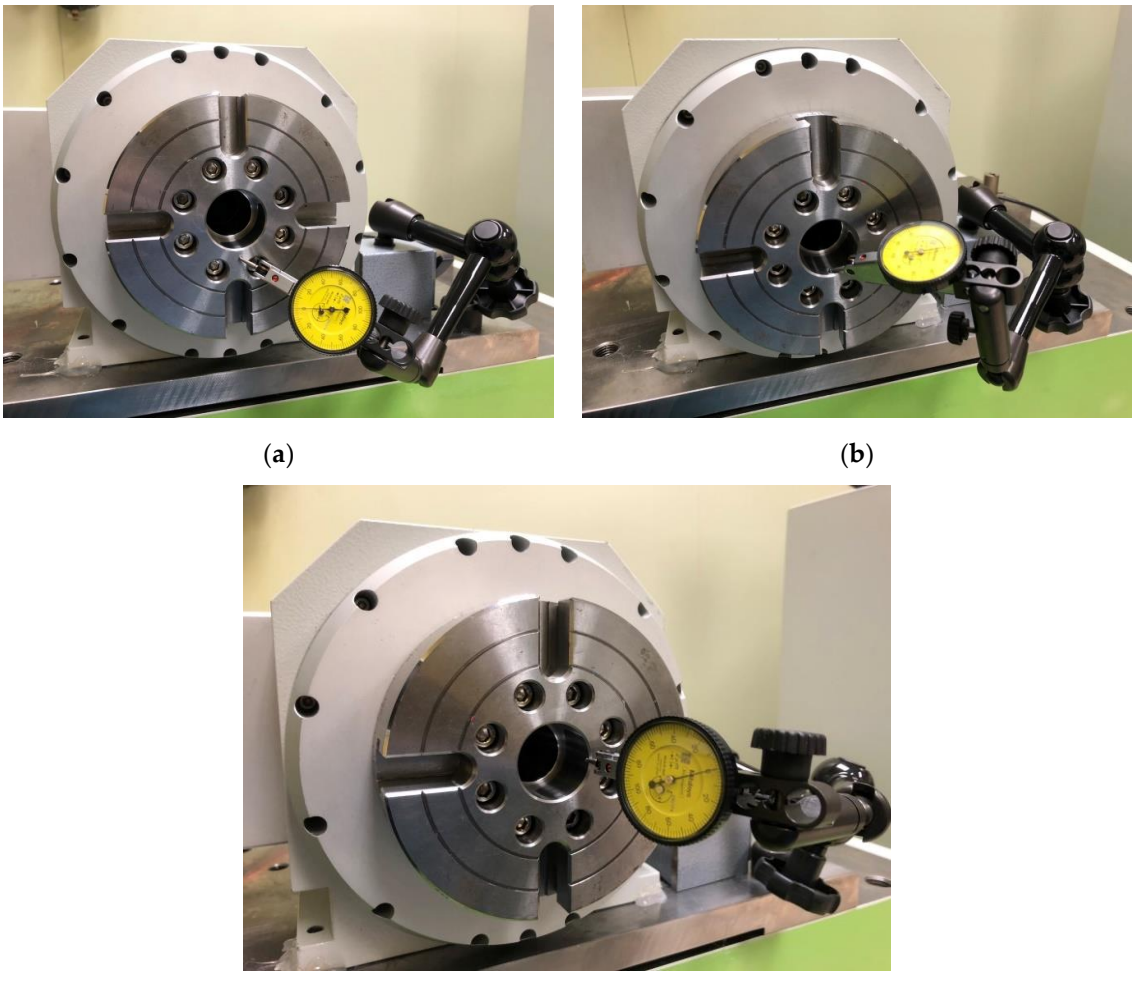

(**a**) (**b**)

(**c**)

Figure 6. Experimental setup for using dial indicator measurement: (**a**) in x direction, (**b**) in y direction, and (**c**) in z direction, respectively.

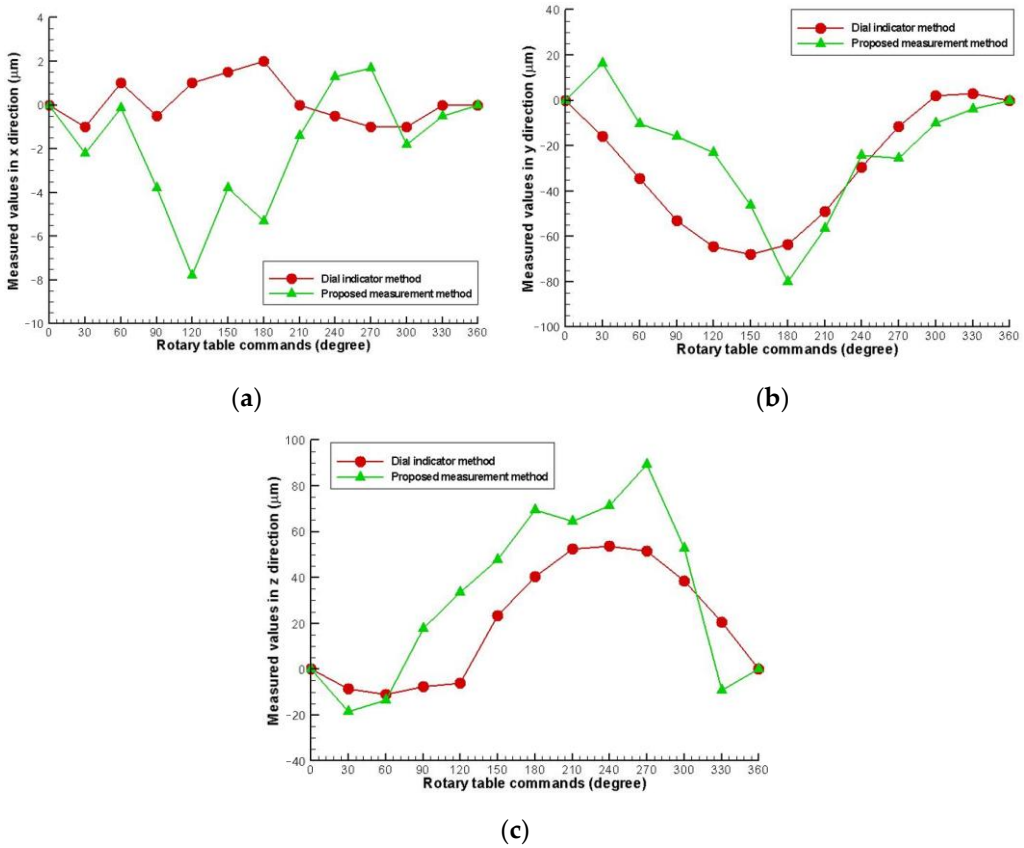

Figure 7. Comparative test results: (**a**) in x direction, (**b**) in y direction, and (**c**) in z direction, respectively.

6. Conclusions

As a basis for enhancing the accuracy of the rotary table, this paper proposed a robust measurement method for the identification and calibration of 6-DOF geometric errors in rotary tables by using LaserTRACER and reflectors. The specific characteristic of the proposed measurement method was that it can be executed to measure the 6-DOF geometric errors of a rotary table without driving the other three external linear axes. To improve the measurement accuracy of 6-DOF geometric errors of a rotary table, a measurement algorithm for reducing the set-up errors that influence the measurement value was also considered and established. As a result, the proposed measurement method had the advantages of efficiency and convenience. From the obtained simulation verification results of set-up errors, the maximal relative differences in the linear offset errors and angular errors were equal to, at most, 4.5% and 4.35%, respectively. Moreover, the simulation verification results of the 6-DOF geometric errors indicated that the maximal relative differences in the linear errors and the angular errors were, at most, 3.25% and 2.30%, respectively. On the other hand, the experiment of the proposed measurement system was also executed for verifying its feasibility and performance. According to the experimental results, the maximum linear offset error and angular error were 192.6 μm and 108.70 arcsec, respectively. Conclusively, the experiment and simulation verification results demonstrated that the 6-DOF geometric errors of rotary tables can be identified precisely by using the proposed measurement method. Finally, it must be emphasized that the proposed method can be applied to any other rotary table configuration.

Author Contributions: Conceptualization, Y.-T.C. and J.-R.C.; methodology, Y.-T.C.; software, C.-H.H.; validation, C.-H.H., J.-R.C. and F.-H.H.; resources, Y.-T.C.; data curation, C.-H.H.; writing—original draft preparation, C.-H.H.; writing—review and editing, Y.-T.C. and F.-H.H.; supervision,

Y.-T.C.; project administration, Y.-T.C.; funding acquisition, Y.-T.C. All authors have read and agreed to the published version of the manuscript.

Funding: This research was funded by the National Science and Technology Council of Taiwan under Grant Nos. NSTC 111−2222−E−150−002− and MOST 111−2218−E−002−032−, as well as by the Bureau of Standards, Metrology and Inspection (BSMI) in Taiwan.

Institutional Review Board Statement: Not applicable.

Informed Consent Statement: Not applicable.

Data Availability Statement: Not applicable.

Conflicts of Interest: The authors declare no conflict of interest.

References

1. Varga, J.; Tóth, T.; Kaščák, Ľ.; Spišák, E. The Effect of the Machining Strategy on the Surface Accuracy When Milling with a Ball End Cutting Tool of the Aluminum Alloy Alcu4mg. *Appl. Sci.* **2022**, *12*, 10638. [CrossRef]
2. Ni, M.; Ni, N.; Liu, H.; Jiang, L.; Mo, W. Design Optimization for the Coating of Machine Tools Based on Eye-Tracking Experiments and Virtual Reality Technology. *Appl. Sci.* **2022**, *12*, 10640. [CrossRef]
3. Yang, X.; You, Y. Linear Tool Path-Smoothing Method in High-Speed Machining Based on Error Feasible Area and Curvature Optimization. *Appl. Sci.* **2022**, *12*, 9443. [CrossRef]
4. Stan, S.-D.; Popişter, F.; Oarcea, A.; Ciudin, P. Comparative Study Using Cad Optimization Tools for the Workspace of a 6dof Parallel Kinematics Machine. *Appl. Sci.* **2022**, *12*, 9258. [CrossRef]
5. Li, B.; Zhang, H.; Ye, P. Error Constraint Optimization for Corner Smoothing Algorithms in High-Speed Cnc Machine Tools. *Int. J. Adv. Manuf. Technol.* **2018**, *99*, 635–646. [CrossRef]
6. Tsutsumi, M.; Saito, A. Identification of Angular and Positional Deviations Inherent to 5-Axis Machining Centers with a Tilting-Rotary Table by Simultaneous Four-Axis Control Movements. *Int. J. Mach. Tools Manuf.* **2004**, *44*, 1333–1342. [CrossRef]
7. Chen, Y.-T.; More, P.; Liu, C.-S. Identification and Verification of Location Errors of Rotary Axes on Five-Axis Machine Tools by Using a Touch-Trigger Probe and a Sphere. *Int. J. Adv. Manuf. Technol.* **2019**, *100*, 2653–2667. [CrossRef]
8. Jeong, J.H.; Khim, G.; Oh, J.S.; Chung, S.-C. Method for Measuring Location Errors Using a Touch Trigger Probe on Four-Axis Machine Tools. *Int. J. Adv. Manuf. Technol.* **2018**, *99*, 1003–1012. [CrossRef]
9. Zha, J.; Li, L.; Han, L.; Chen, Y. Four-Station Laser Tracer-Based Geometric Error Measurement of Rotary Table. *Meas. Sci. Technol.* **2020**, *31*, 065008. [CrossRef]
10. Ibaraki, S.; Oyama, C.; Otsubo, H. Construction of an Error Map of Rotary Axes on a Five-Axis Machining Center by Static R-Test. *Int. J. Mach. Tools Manuf.* **2011**, *51*, 190–200. [CrossRef]
11. Xiang, S.; Yang, J. Using a Double Ball Bar to Measure 10 Position-Dependent Geometric Errors for Rotary Axes on Five-Axis Machine Tools. *Int. J. Adv. Manuf. Technol.* **2014**, *75*, 559–572. [CrossRef]
12. *ISO 230-1:2012*; Test Code for Machine Tools—Part 1: Geometric Accuracy of Machines Operating under No-Load or Quasi-Static Conditions. International Organization for Standardization: Geneva, Switzerland, 2012.
13. *ISO 230-7: 2015*; Test Code for Machine Tools—Part 7: Geometric Accuracy of Axes of Rotation. International Organization for Standardization: Geneva, Switzerland, 2015.
14. Lee, K.-I.; Yang, S.-H. Robust Measurement Method and Uncertainty Analysis for Position-Independent Geometric Errors of a Rotary Axis Using a Double Ball-Bar. *Int. J. Mach. Tools Manuf.* **2013**, *14*, 231–239. [CrossRef]
15. *ISO 10791-1:2015*; Test Conditions for Machining Centres—Part 1: Geometric Tests for Machines with Horizontal Spindle (Horizontal Z-Axis). International Organization for Standardization: Geneva, Switzerland, 2015.
16. *ISO 10791-2:2001*; Test Conditions for Machining Centres—Part 2: Geometric Tests for Machines with Vertical Spindle or Universal Heads with Vertical Primary Rotary Axis (vertical Z-Axis). International Organization for Standardization: Geneva, Switzerland, 2001.
17. *ISO 10791-3:1998*; Test Conditions for Machining Centres—Part 3: Geometric Tests for Machines with Integral Indexable or Continuous Universal Heads (Vertical Z-Axis). International Organization for Standardization: Geneva, Switzerland, 1998.
18. *ISO 10791-6:2014*; Test Conditions for Machining Centres—Part 6: Accuracy of Speeds and Interpolations. International Organization for Standardization: Geneva, Switzerland, 2014.
19. Chen, Y.-T.; More, P.; Liu, C.-S.; Cheng, C.-C. Identification and Compensation of Position-Dependent Geometric Errors of Rotary Axes on Five-Axis Machine Tools by Using a Touch-Trigger Probe and Three Spheres. *Int. J. Adv. Manuf. Technol.* **2019**, *102*, 3077–3089. [CrossRef]
20. Ibaraki, S.; Iritani, T.; Matsushita, T. Calibration of Location Errors of Rotary Axes on Five-Axis Machine Tools by on-the-Machine Measurement Using a Touch-Trigger Probe. *Int. J. Mach. Tools Manuf.* **2012**, *58*, 44–53. [CrossRef]
21. Liu, C.-S.; Hsu, H.-C.; Lin, Y.-X. Design of a Six-Degree-of-Freedom Geometric Errors Measurement System for a Rotary Axis of a Machine Tool. *Opt. Lasers Eng.* **2020**, *127*, 105949. [CrossRef]

22. Schwenke, H.; Knapp, W.; Haitjema, H.; Weckenmann, A.; Schmitt, R.; Delbressine, F. Geometric Error Measurement and Compensation of Machines—An Update. *CIRP Ann. Manuf. Technol.* **2008**, *57*, 660–675. [CrossRef]
23. Ibaraki, S.; Knapp, W. Indirect Measurement of Volumetric Accuracy for Three-Axis and Five-Axis Machine Tools: A Review. *Int. J. Mach. Tools Manuf.* **2012**, *6*, 110–124. [CrossRef]
24. Jiang, X.; Cripps, R.J. A Method of Testing Position Independent Geometric Errors in Rotary Axes of a Five-Axis Machine Tool Using a Double Ball Bar. *Int. J. Mach. Tools Manuf.* **2015**, *89*, 151–158. [CrossRef]
25. Xia, H.-J.; Peng, W.-C.; Ouyang, X.-B.; Chen, X.-D.; Wang, S.-J.; Chen, X. Identification of Geometric Errors of Rotary Axis on Multi-Axis Machine Tool Based on Kinematic Analysis Method Using Double Ball Bar. *Int. J. Mach. Tools Manuf.* **2017**, *122*, 161–175. [CrossRef]
26. Ibaraki, S.; Iritani, T.; Matsushita, T. Error Map Construction for Rotary Axes on Five-Axis Machine Tools by on-the-Machine Measurement Using a Touch-Trigger Probe. *Int. J. Mach. Tools Manuf.* **2013**, *68*, 21–29. [CrossRef]
27. He, Z.; Fu, J.; Zhang, L.; Yao, X. A New Error Measurement Method to Identify All Six Error Parameters of a Rotational Axis of a Machine Tool. *Int. J. Mach. Tools Manuf.* **2015**, *88*, 1–8. [CrossRef]
28. Li, J.; Feng, Q.; Bao, C.; Zhao, Y. Method for Simultaneous Measurement of Five Dof Motion Errors of a Rotary Axis Using a Single-Mode Fiber-Coupled Laser. *Opt. Express* **2018**, *26*, 2535–2545. [CrossRef] [PubMed]
29. Muralikrishnan, B.; Lee, V.; Blackburn, C.; Sawyer, D.; Phillips, S.; Ren, W.; Hughes, B. Assessing Ranging Errors as a Function of Azimuth in Laser Trackers and Tracers. *Meas. Sci. Technol.* **2013**, *24*, 065201. [CrossRef]
30. Lee, H.-W.; Chen, J.-R.; Pan, S.-P.; Liou, H.-C.; Hsu, P.E. Relationship between Iso 230-2/-6 Test Results and Positioning Accuracy of Machine Tools Using Lasertracer. *Appl. Sci.* **2016**, *6*, 105. [CrossRef]
31. Chen, J.R.; Ho, B.-L.; Lee, H.-W.; Pan, S.-P.; Hsieh, T.-H. Geometric Error Measurement of Machine Tools Using Autotracking Laser Interferometer. *Sens. Mater.* **2018**, *30*, 2429. [CrossRef]
32. Zhang, Z.; Hu, H. A General Strategy for Geometric Error Identification of Multi-Axis Machine Tools Based on Point Measurement. *Int. J. Adv. Manuf. Technol.* **2013**, *69*, 1483–1497. [CrossRef]
33. Haitao, L.; Junjie, G.; Yufen, D.; Jindong, W.; Xinrong, H. Identification of Geometric Deviations Inherent to Multi-Axis Machine Tools Based on the Pose Measurement Principle. *Meas. Sci. Technol.* **2016**, *27*, 125008. [CrossRef]
34. Wang, J.; Guo, J. The Identification Method of the Relative Position Relationship between the Rotary and Linear Axis of Multi-Axis Numerical Control Machine Tool by Laser Tracker. *Meas. Sci. Technol.* **2019**, *132*, 369–376. [CrossRef]
35. Schwenke, H.; Franke, M.; Hannaford, J.; Kunzmann, H. Error Mapping of Cmms and Machine Tools by a Single Tracking Interferometer. *CIRP Ann. Manuf. Technol.* **2005**, *54*, 475–478. [CrossRef]
36. Hughes, E.B.; Wilson, A.; Peggs, G.N. Design of a High-Accuracy Cmm Based on Multi-Lateration Techniques. *CIRP Ann. Manuf. Technol.* **2000**, *49*, 391–394. [CrossRef]
37. Muralikrishnan, B.; Phillips, S.; Sawyer, D. Laser Trackers for Large-Scale Dimensional Metrology: A Review. *Precis. Eng.* **2016**, *44*, 13–28. [CrossRef]
38. Gąska, A.; Krawczyk, M.; Kupiec, R.; Ostrowska, K.; Gąska, P.; Sładek, J. Modeling of the Residual Kinematic Errors of Coordinate Measuring Machines Using Lasertracer System. *Int. J. Adv. Manuf. Technol.* **2014**, *73*, 497–507. [CrossRef]
39. Wang, J.; Guo, J.; Zhang, G.; Guo, B.A.; Wang, H. The Technical Method of Geometric Error Measurement for Multi-Axis Nc Machine Tool by Laser Tracker. *Meas. Sci. Technol.* **2012**, *23*, 045003. [CrossRef]
40. Toshiyuki, T.; Yoshihiko, K.; Mitsuo, G.; Tomizo, K. Restriction on the Arrangement of Laser Trackers in Laser Trilateration. *Meas. Sci. Technol.* **1998**, *9*, 1357.
41. Toshiyuki, T.; Mitsuo, G.; Tomizo, K.; Yoshihisa, T.; Yoshihiko, K. The First Measurement of a Three-Dimensional Coordinate by Use of a Laser Tracking Interferometer System Based on Trilateration. *Meas. Sci. Technol.* **1998**, *9*, 38.
42. *ISO/IEC Guide 98-3:2008*; Uncertainty of Measurement—Part 3: Guide to the Expression of Uncertainty in Measurement (GUM:1995). International Organization for Standardization: Geneva, Switzerland, 2008.
43. *ISO 13528: 2015*; Statistical Methods for Use in Proficiency Testing by Interlaboratory Comparison. International Organization for Standardization: Geneva, Switzerland, 2015.